THE UNIVERSITY of EDINBURGH

Edinburgh Research Explorer

Long-range, critical-point dynamics in oil field flow rate data

OPEN ACCESS

Long-range, critical-point dynamics in oil field flow rate data

I. G. Main,[1] L. Li,[1] K. J. Heffer,[2] O. Papasouliotis,[3,4] and T. Leonard[3]

[1] Earthquake triggering data exhibit long-range spatio-temporal correlations of the power-law form $C(l) \sim l^{-\alpha}$ and anomalously-slow temporal diffusion of the mean triggering distance of the form: $\langle l \rangle \sim t^H$, with $H < 0.5$. We examine spatio-temporal correlations in subsurface effective stress state caused by fluid injection and extraction at well sites in a hydrocarbon reservoir using a multivariate statistical regression model, and observe long-range correlations in flow rate that cannot be caused by Darcy flow alone. Significantly-correlated well pairs align with the directions of incipient horizontal-displacement tensile and shear failure in the present-day stress field, while the contours of the first principal component of the regression matrix closely follow the macroscopic fault pattern in the main producing horizon. The correlation function for well pairs has a power-law form with $\alpha \approx 0.5$, and the mean correlation distance increases with $H \approx 0.33$, implying a similar critical-point response to perturbations in effective stress as the earthquake data. **Citation:** Main, I. G., L. Li, K. J. Heffer, O. Papasouliotis, and T. Leonard (2006), Long-range, critical-point dynamics in oil field flow rate data, *Geophys. Res. Lett.*, *33*, L18308, doi:10.1029/2006GL027357.

1. Introduction

[2] There has been a significant debate on the mechanism of earthquake-earthquake triggering [*Stein et al.*, 1992; *Stein*, 1999; *Voisin et al.*, 2004; *Steacy et al.*, 2005; *Parsons*, 2005; *Felzer and Brodsky* 2006; *Main*, 2006], largely prompted by the very long-range triggering that followed the 1992 Landers earthquake in California [*Hill et al.*, 1993; *Stark and Davis*, 1996]. After that event micro-earthquakes began in hydrothermal fields at distances quite remote from the main-shock, immediately after the passage of the Rayleigh wave, indicating a dynamic triggering mechanism. Others have argued instead for a significant component of static (Coulomb) stress mechanism [*Stein et al.*, 1992; *Stein*, 1999]. In either case the predicted stress perturbations are much smaller than the earthquake stress drop [*Nalbant et al.*, 2005], implying a pre-existing sensitivity of the triggered area to a small stress change. This may be due to (a) a significant non-linear amplification effect, such as the rate-dependent term in the rate and state friction law [*Stein*, 1999; *Parsons*, 2005] and/or (b) the crust already being primed to a critical state [*Cowie et al.*, 1993; *Helmstetter et al.*, 2003].

[3] Several studies have highlighted the role of local changes in pore pressure (of magma or hydrothermal fluids) as a stress amplification effect for earthquake triggering [*Stark and Davis*, 1996; *Johnston et al.*, 1995; *Linde and Sacks*, 1998]. Similarly it is well known that changes in pore pressure may also induce seismic events, either due to dam impoundment at the surface [*Talwani*, 1997], or to fluids extracted or injected by boreholes [*Segall*, 1989; *Rutledge et al.*, 1998]. Here we examine a third possibility of examining long-range correlation in the poro-mechanical response of the crust by using direct data on fluid-fluid correlations between boreholes.

[4] One way of checking for critical-point dynamics in the transient response of the brittle lithosphere to stress perturbation is to evaluate the correlation function $C(l)$, i.e. the probability of an event being triggered at a distance l, up to some time t after the triggering event. Using a stacking technique to eliminate the random background seismicity several authors [*Marsan et al.*, 2000; *Huc and Main*, 2003; *McKernon and Main*, 2005] have recently showed $C(l) \sim l^{-\alpha}$, i.e. the power-law form of correlation function expected for a system near the critical point, with strong sensitivity to small stress perturbations [*Main*, 1996]. The stacked results also show an exponential tail, indicating a correlation length of a few tens of km, i.e. the same order of magnitude as the local seismogenic thickness [*Huc and Main*, 2003; *McKernon and Main*, 2005]. A similar power-law correlation function was observed by *Felzer and Brodsky* [2006] with no sign of an exponential tail up to a distance of 50 km or so. For the Centroid Moment Tensor and International Seismological Centre global earthquake catalogues the mean triggering distance for shallow earthquakes increases with time as $\langle l \rangle \sim t^H$, with $H \approx 0.1$, much smaller than that expected for either a solitary wave ($H = 1$) or a Fickian diffusion process ($H = 0.5$) [*Huc and Main*, 2003; *McKernon and Main*, 2005]. The observed anomalously slow diffusion is likely to be related to the strong influence of a pre-existing localization of elastic properties associated with a fault network near the critical point [*Helmstetter et al.*, 2003]. If such features can be seen in natural earthquake data, it might be expected that they may also occur when the effective stress field in the subsurface is perturbed by anthropogenic changes in pore fluid pressure. Here we examine the spatio-temporal correlation function for fluid injection and extraction in a test case oil field in the North Sea, using water or gas injection and oil production well flow rate data.

2. Methods

[5] To determine the response of the subsurface to perturbations we minimize the prediction error

$$\varepsilon = \sum_{t=2}^{T} \sum_{i=1}^{N} \left(y_{i,t} - \hat{y}_{i,t} \right)^2 \tag{1}$$

---

[1]School of GeoSciences, University of Edinburgh, Edinburgh, UK.
[2]Institute of Petroleum Engineering, Heriot-Watt University, Edinburgh, UK.
[3]School of Mathematics and Statistics, University of Edinburgh, Edinburgh, UK.
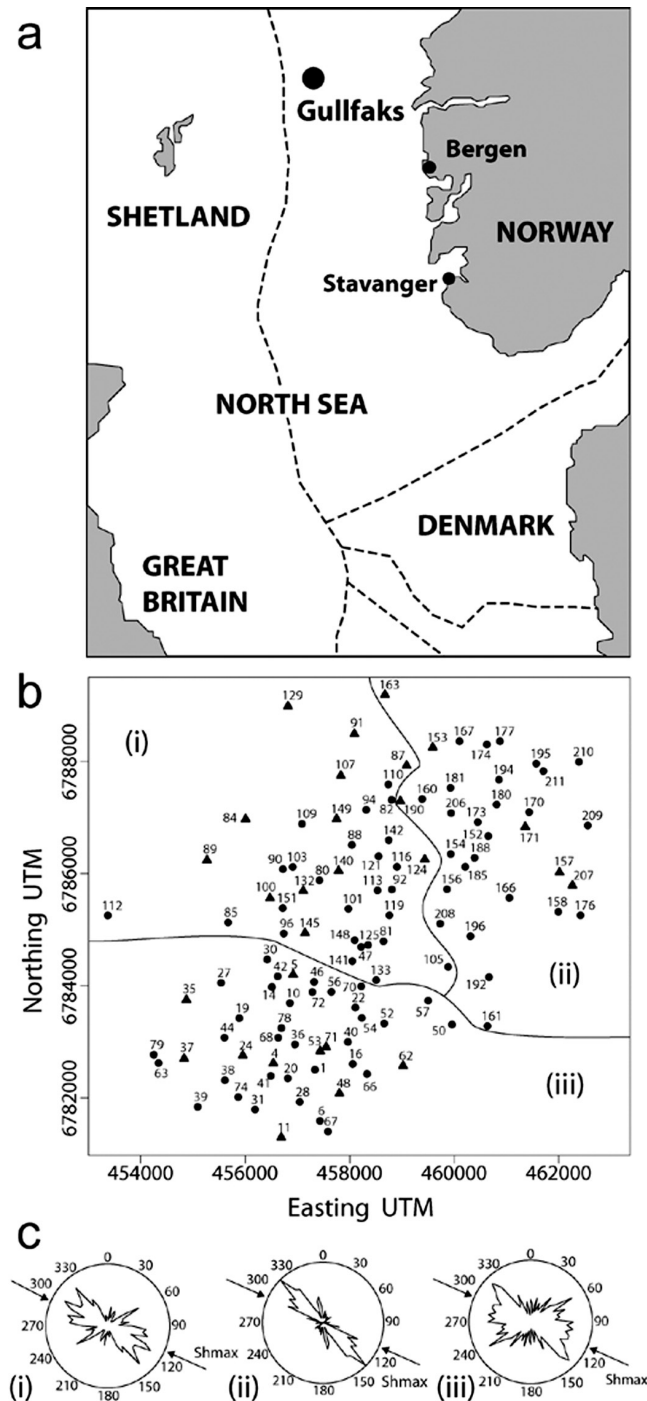[4]Now at Serono International, Geneva, Switzerland.

Figure 1. (a) Location of the Gullfaks oil field. (b) Location of numbered Producers (circles) and Injectors (triangles) subdivided into three regions associated with platforms (i), (ii), and (iii). (c) Rose diagrams of the orientation distribution of significantly-correlated well pairs for zones (i), (ii), and (iii), each compared with the orientation of the regional maximum horizontal principal stress (Shmax - N110E ± 16 from World Stress Map data).

between the observed fluid flow rate $y_{i,t}$ at the i'th producer for times $t = 2, \ldots, T$ and that predicted, $\hat{y}_{i,t}$, by multivariate regression on a vector X_{t-k} of elements comprising the flow rates $x_{j,t-k}$ at all N producers and M injectors at time $t-k$, where k is a lag time. The solution to (1) for all $y_{i,t}$ is the Statistical Reservoir Model

$$\hat{Y}_t = R_k X_{t-k}, \tag{2}$$

where $\hat{Y}_t$ is a vector of predicted flow rates at all N producers and R_k is a matrix of the regression parameters. For more than one time lag R_k would be a three-dimensional array with elements $r_{i,j,k}$: $i = 1, \ldots, N; j = 1, \ldots, N + M; k = 1, \ldots, K$.

[6] The inversion for the optimal Statistical Reservoir Model is done in two steps [*Papasouliotis*, 2000] (detailed in UK patent application 0524134.4, filed 26/11/2005). First the well pairs that are significantly correlated at different lag times are identified using a Bayesian Information Criterion (BIC) (*Papasouliotis* [2000], modified after *Leonard and Hsu* [1999, equation 1.1.6]). This removes well pairs that do not significantly contribute information. Pragmatically the search is stopped for a given producer when the multivariate regression coefficient is $R^2 = 0.99$. Second, Bayesian Dynamic Linear Modelling (*Papasouliotis* [2000] based on models presented by *Leonard and Hsu* [1999, sections 5.5 and 5.6] is used to eliminate a lower number of pairs whose optimal regression slope is not significantly different from zero. These two steps together define a binary significance matrix, S_{ij}, where most elements are zero, resulting in a parsimonious model. Typically only 5–25 out of the 106 wells in the field are needed to achieve $R^2 = 0.99$ for a given producer.

[7] Data were provided as monthly averages and treated as time series. For those well pairs identified as significant, $S_{ij} = 1$, we then calculate the optimal regression model R_{ij} using (1). Optimal time lags of $k = 0$ and $k = 1$ month were determined by examining the goodness of fit of the resulting time series. A more detailed analysis to be presented elsewhere reveals that some predictive power may also exist at higher lags (a few months), but at decreasing resolution. These timescales reveal both a direct (instantaneous) effect, consistent with the poroelastic mechanism for stress transfer on fluid injection or withdrawal [*Segall*, 1989], and a time-dependent effect of the order of one or a few months, the latter similar to that seen in earthquake aftershock sequences or induced seismicity.

[8] Principal component (PC) analysis is commonly used to extract spatial information from multivariate point sampling data, for example to infer past permeability and deformation fields in mineral prospecting [*Reyment and Joreskog*, 1996]. Put simply PC analysis "creates a minimum number of new variables, which are linear combinations of the original ones such that the new variables contain most or all of the information" [*Reyment and Joreskog*, 1996]. The degree of information associated with each principal component, or eigenvector, of the correlation matrix is represented by its corresponding eigenvalue. To exclude imaginary eigenvalues, only the symmetric component of the matrix S_{ij} is decomposed into its eigensolutions, by conventional linear algebra [*Reyment and Joreskog*, 1996]. Here we examine the principal component corresponding to the largest eigenvalue. The principal component has values at
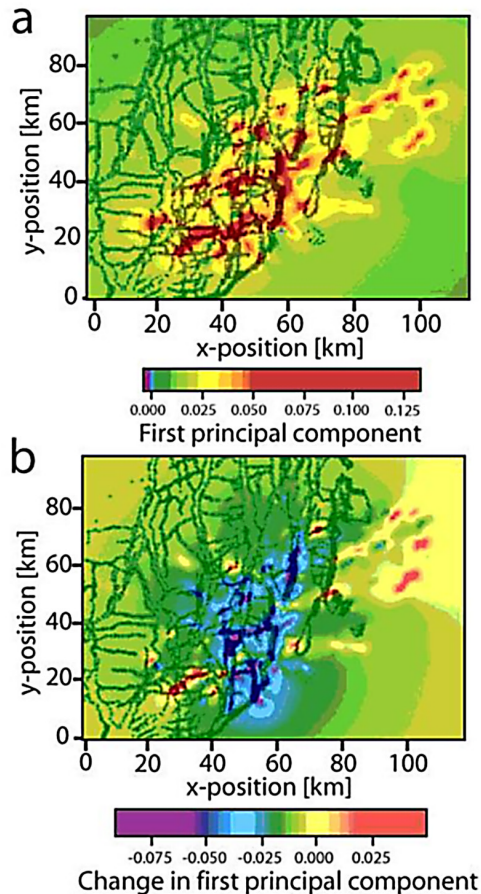
Figure 2. (a) The first principal component (PC1) from the significance matrix $S_{i,j}$ for either zero or one month lags, compared with the seismically-imaged fault pattern (lines) at the top Etive producing horizon in the Gullfaks field for the first 133 months of production data. (b) Change in amplitude of PC1 from 67 to 133 months of production data.

a subset of the well locations: values between those locations were interpolated using the spatial correlation functions described by *Heffer and King* [2006], prior to contouring the data.

3. Results

[9] We examine the correlation function for flow rate at injectors and producers in an oil field, using data for the Gullfaks field in the North Sea (Figure 1a). Using the method described above we solve for the binary significance matrix $S_{i,j}$ and a real regression matrix $R_{i,j}$ for a given time lag k. Each well pair with $S_{i,j} = 1$ at either zero or one month lag is associated with a vector $l_{i,j}$ of orientation $\theta_{i,j}$ and scalar length $l_{i,j}$ determined from the relative location at the main producing horizon.

[10] Figure 1 shows polar plots of $\theta_{i,j}$ for the significantly-correlated well pairs using the first 133 months of production data. The data is split into three zones representing the three platforms used to operate the field, and show some spatial variation around the dominant trends. However, all zones

have a strong sub-parallel alignment of preferred azimuth $\theta_{i,j}$ with respect to the direction of maximum principal horizontal stress, i.e. the orientation of tensile fracture in the present-day stress field. This match has previously been observed on other fields using the Spearman rank correlation method at zero time lag [*Heffer et al.*, 1995]. Our results also show some preferred orientations at around 30 degrees or so to the tensile orientation, implying a response also in the directions of incipient shear (Coulomb) failure in strike-slip mode. The inference of enhanced flow at incipient failure is consistent with the dilatancy observed at near-critical conditions in laboratory tests of rough surfaces undergoing shear [*Zimmermann and Main*, 2004], as previously inferred from borehole micro-thermometry in other oil fields [*Barton et al.*, 1995].

[11] Figure 2a plots interpolated contours for the first principal component of the symmetric component of the matrix $S_{i,j}$, superposed on the faulting pattern within the main producing horizon. The results, derived from only the flow rate data themselves, correlate well with some of the main faults in the field, in location, extent and orientation, in particular picking up the long-range grid-like pattern associated with fault trends due to much earlier deformation events in the NNW-SSE and ENE-WSW directions. The principal component patterns evolve with duration of production. Their association with faulting becomes more striking when the map of the difference in the first principal component between an intermediate and the final time of analysis is superposed on the fault pattern (Figure 2b). The results confirm that the underlying long-range fault structure plays an immediate and significant role in controlling reservoir response to pore pressure transients associated with flow rate changes, consistent with the inference of a strong control of pre-existing faulting pattern on natural stress transients from triggered seismicity [*Helmstetter et al.*, 2003].

[12] Figure 3 shows the correlation function $C(l)$ for $S_{ij} = 1$, normalized for the initial distribution of all possible well spacings. Apart from the shortest and longest distances, where the spatial sampling in the normalization is weakest, the results show long range correlations of power-law form,
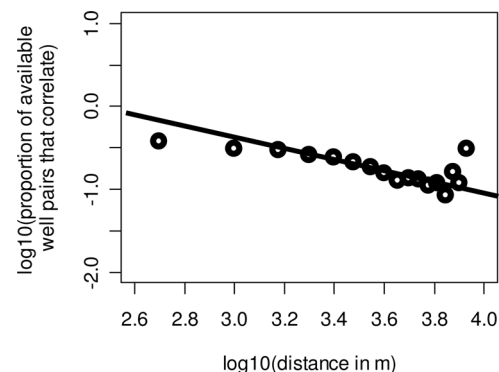

Figure 3. The number of correlated pair wells at a given distance normalized by available wells at that separation as a function of distance for the first 85 months production in the Gullfaks field. The normalized number of correlated pair wells is shown by circles, and the best power law fit by straight line, with negative slope $\alpha \approx 0.5$.
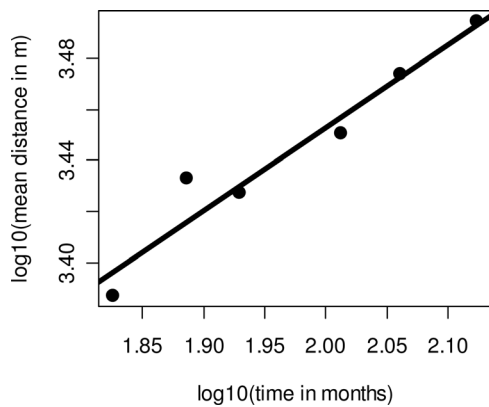
Figure 4. Evolution of mean distance $\langle l \rangle (t)$ for times t varying between 67 and 133 months, for the significantly correlated well pairs in the Gullfaks field. The best power law fit $R(t) \sim t^H$ (solid line) has an exponent $H = 0.33$.

with an exponent $\alpha \approx 0.5$ and no sign of a finite correlation length within the largest distance determined by the size of the field ($\approx$10km). This is consistent with a correlation length of at least the same order of magnitude as the brittle thickness of the lithosphere, as observed in the earthquake triggering data cited above. The mean triggering distance (for zero or one month lag) increases with the duration of the time window as a power law with $H \approx 0.33$ (Figure 4), indicating anomalous diffusion, also consistent with the earthquake data described in the introduction.

[13] The long-range correlations revealed by Figures 2 and 3, are consistent with a critical point response to perturbation of the pore pressure [*Maillot et al.*, 1999]. More specific recent numerical simulations based on the architecture of the main faults in the Gullfaks oil field confirm that long-range correlations of the type we observe here could be produced by hydraulically-reactive faults and fractures, but only in a pre-existing critically-stressed medium where a strong non-linearity is introduced in the form of large changes in permeability with respect to effective stress [*Zhang et al.*, 2006].

4. Conclusion

[14] We observe long-range correlations in subsurface fluid flow rate at well sites that are sensitive both to the present-day stress field and the pre-existing fault architecture, have a power-law correlation function, and exhibit anomalous diffusion. All of these attributes are common to key observations in natural or induced triggered seismicity. Our results can be explained most easily by the combined mechanical and hydraulic response of a near-critical reservoir to local perturbations in effective stress. Key elements are the existence of a pre-existing set of faults and fractures that dominate the flow heterogeneity, a present-day anisotropic stress field that is near-critical, a long-range tensile or Coulomb response to fluid pressure change, and strong feedback between effective stress and permeability. The similarity in many respects to naturally-triggered earthquakes suggests in turn that non-linear feedbacks between present-day stress, porosity, permeability, deformation and fluid flow,

superposed on previous geological structure, may also play a significant combined role in natural earthquake dynamics.

References

Barton, C. A., M. D. Zoback, and D. Moos (1995), Fluid flow along potentially active faults in crystalline rock, *Geology*, *23*, 683–686.

Cowie, P. A., C. Vanneste, and D. Sornette (1993), Statistical physics model for the spatio-temporal evolution of faults, *J. Geophys. Res.*, *98*, 21,809–21,821.

Felzer, K. R., and E. E. Brodsky (2006), Decay of aftershock density with distance indicates triggering by dynamic stress, *Nature*, *441*, 735–738.

Heffer, K. J., R. J. Fox, C. A. McGill, and N. C. Koutsebaloulis (1995), Novel techniques show links between reservoir flow directionality, Earth stress, fault structure, and geomechanical changes in mature waterfloods, *SPE Pap. 30711*, Soc. of Pet. Eng., Richardson, Tex.

Heffer, K., and P. King (2006), Spatial scaling of effective modulus and correlation of deformation near the critical point of fracturing, *Pure Appl. Geophys.*, in press.

Helmstetter, A., G. Ouillon, and D. Sornette (2003), Are aftershocks of large Californian earthquakes diffusing?, *J. Geophys. Res.*, *108*(B10), 2483, doi:10.1029/2003JB002503.

Hill, D. P., et al. (1993), Seismicity in the western United States remotely triggered by the M 7.4 Landers, California, earthquake of June 28, 1992, *Science*, *260*, 1617–1623.

Huc, M., and I. G. Main (2003), Anomalous stress diffusion in earthquake triggering: Correlation length, time dependence, and directionality, *J. Geophys. Res.*, *108*(B7), 2324, doi:10.1029/2001JB001645.

Johnston, M. J. S., D. P. Hill, J. Linde, A. T. Langbein, and R. Bilham (1995), Transient deformation during triggered seismicity from the 28 June 1992 Mw = 7.3 Landers earthquake at Long Valley Volcanic Caldera, California, *Bull. Seismol. Soc. Am.*, *85*, 787–795.

Leonard, T., and J. S. J. Hsu (1999), *Bayesian Methods*, Cambridge Univ. Press, New York.

Linde, A. T., and I. S. Sacks (1998), Triggering of volcanic eruptions, *Nature*, *395*, 888–890.

Maillot, B., S. Nielsen, and I. Main (1999), Numerical simulation of seismicity due to fluid injection in a brittle poro-elastic medium, *Geophys. J. Int.*, *139*, 263–272.

Main, I. G. (1996), Statistical physics, seismogenesis, and seismic hazard, *Rev. Geophys.*, *34*, 433–462.

Main, I. G. (2006), A hand on the aftershock trigger, *Nature*, *441*, 704–705.

Marsan, D., C. J. Bean, S. Steacy, and J. McCloskey (2000), Observation of diffusion processes in earthquake populations and implications for the predictability of seismicity systems, *J. Geophys. Res.*, *105*, 28,081–28,094.

McKernon, C., and I. G. Main (2005), Regional variations in the diffusion of triggered seismicity, *J. Geophys. Res.*, *110*, B05S05, doi:10.1029/2004JB003387.

Nalbant, S. S., S. Steacy, K. Sieh, D. Natawidjaja, and J. McCloskey (2005), Earthquake risk on the Sunda trench, *Nature*, *435*, 756–757.

Papasouliotis, O. (2000), Spatio-temporal models for oil well pressures, in *Statistical Methods for the Analysis of Covariance and Spatio-temporal Models*, Ph.D. thesis, chap. 5, pp. 121–140, Univ. of Edinburgh, Edinburgh, U. K.

Parsons, T. (2005), A hypothesis for delayed dynamic earthquake triggering, *Geophys. Res. Lett.*, *32*, L04302, doi:10.1029/2004GL021811.

Reyment, R., and K. G. Joreskog (1996), *Applied Factor Analysis in the Natural Sciences*, 2nd ed., p. 4, Cambridge Univ. Press, New York.

Rutledge, J. T., W. S. Phillips, and B. K. Schuessler (1998), Reservoir characterization using oil-production-induced microseismicity, Clinton County, Kentucky, *Tectonophysics*, *289*, 129–152.

Segall, P. (1989), Earthquakes triggered by fluid extraction, *Geology*, *17*, 942–946.

Stark, M. A., and S. D. Davis (1996), Remotely triggered microearthquakes at the Geysers geothermal field, California, *Geophys. Res. Lett.*, *23*, 945–948.

Steacy, S., J. Gomberg, and M. Cocco (2005), Introduction to special section: Stress transfer, earthquake triggering, and time-dependent seismic hazard, *J. Geophys. Res.*, *110*, B05S01, doi:10.1029/2005JB003692.

Stein, R. (1999), The role of stress transfer in earthquake occurrence, *Nature*, *402*, 605–609.

Stein, R., G. C. P. King, and J. Lin (1992), Change in failure stress on the southern San Andreas fault system caused by the 1992 Magnitude = 7.4 Landers earthquake, *Science*, *258*, 1328–1332.

Talwani, P. (1997), On the nature of reservoir-induced seismicity, *Pure Appl. Geophys.*, *150*, 473–492.

Voisin, C., F. Cotton, and S. Di Carli (2004), A unified model for dynamic and static stress triggering of aftershocks, antishocks, remote seismicity, creep events, and multisegmented rupture, *J. Geophys. Res.*, *109*, B06304, doi:10.1029/2003JB002886.

Zhang, X., N. Koutsebaloulis, and K. Heffer (2006), Hydro-mechanical modelling of critically-stressed and faulted reservoirs, *AAPG Bull.*, *90*, in press.

Zimmermann, R., and I. Main (2004), in *Mechanics of Fluid-Saturated Rocks*, edited by Y. Gueguen and M. Bouteca, pp. 363–422, Elsevier, New York.

_____

K. J. Heffer, Institute of Petroleum Engineering, Heriot-Watt University, Riccarton Campus, Edinburgh EH14 4AS, UK.

T. Leonard, School of Mathematics and Statistics, University of Edinburgh, Mayfield Road, Edinburgh EH9 3JZ, UK.

L. Li and I. G. Main, School of GeoSciences, University of Edinburgh, West Mains Road, Edinburgh EH9 3JW, UK. (ian.main@ed.ac.uk)

O. Papasouliotis, Serono International, 15bis, chemin des Mines, Case Postale 54, CH-1211 Geneva 20, Switzerland.